Published in final edited form as:
Synapse. 2009 June ; 63(6): 462–475. doi:10.1002/syn.20626.

Pharmacological characterization of 2-methoxy-*N*-propylnorapomorphine's (MNPA) interactions with D_2 and D_3 dopamine receptors

Mette Skinbjerg[a,b,c], **Yoon Namkung**[a], **Christer Halldin**[b], **Robert B. Innis**[c], and **David R. Sibley**[a,d]

[a]Molecular Neuropharmacology Section, National Institute of Neurological Disorders and Stroke, Bethesda, MD, USA

[b]Karolinska Institutet, Department of Clinical Neuroscience, Psychiatry Section, Stockholm, Sweden

[c]Molecular Imaging Branch, National Institute of Mental Health, Bethesda, MD, USA

Abstract

Dopaminergic signaling pathways have been extensively investigated using PET imaging, primarily with antagonist radioligands of D_2 and D_3 dopamine receptors (DARs). Recently, agonist radioligands of D_2/D_3 DARs have begun to be developed and employed. One such agonist is (*R*)-2-$^{11}CH_3O$-*N*-*n*-propylnorapomorphine (MNPA). Here, we perform a pharmacological characterization of MNPA using recombinant D_2 and D_3 DARs expressed in HEK293 cells. MNPA was found to robustly inhibit forskolin-stimulated cAMP accumulation to the same extent as dopamine in D_2 or D_3 DAR-transfected cells, indicating that it is a full agonist at both receptors. MNPA is ~50-fold more potent than dopamine at the D_2 DAR, but equally potent as dopamine at the D_3 DAR. MNPA competition binding curves in membrane preparations expressing D_2 DARs revealed two binding states of high and low-affinity. In the presence of GTP, only one binding state of low affinity was observed. Direct saturation binding assays using [^{3}H]MNPA revealed similar results as with the competition experiments leading to the conclusion that MNPA binds to the D_2 DAR in an agonist-specific fashion. In contrast to membrane preparations, using intact cell binding assays, only one site of low affinity was observed for MNPA and other agonists binding to the D_2 DAR. MNPA was also found to induce D_2 DAR internalization to an even greater extent that dopamine as determined using both cell surface receptor binding assays and confocal fluorescence microscopy. Taken together, our data indicate that the PET tracer, MNPA, is a full and potent agonist at both D_2 and D_3 receptors.

Keywords

MNPA; Dopamine; Receptor; Agonist; Internalization; PET

Introduction

The dopamine receptors (DARs) have been extensively investigated using PET antagonist radioligands, but recently, a number of agonist radioligands have been developed (Cumming et al., 2003; Mukherjee et al., 2004; Willeit et al., 2006; Wilson et al., 2005). Such PET

[d]To whom correspondence should be addressed at: Dr. David R. Sibley, Molecular Neuropharmacology Section, National Institute of Neurological Disorders & Stroke/NIH, 5625 Fishers Lane, Room 4S-04, MSC-9405, Bethesda, MD 20892-9405, Phone: 301-496-9316, Fax: 301-480-3726, Email: sibley@helix.nih.gov.

ligands include (*R*)-2-$^{11}CH_3O$-*N*-*n*-propylnorapomorphine (MNPA), a methoxy derivative of the D_2/D_3 DAR agonist *N*-*n*-propylnorapomorphine (NPA) (Finnema et al., 2005; Gao et al., 1990; Seneca et al., 2006) and [^{11}C]PHNO (Freedman et al., 1994; Ginovart et al., 2006; Narendran et al., 2006; Willeit et al., 2006). An important property of such agonist PET probes, which differentiates them from antagonists, is their ability to induce an activated state of the receptor that is capable of productive interactions with G-proteins. The ability of agonists to promote receptor-G-protein interactions is commonly observed as the existence of a high affinity, guanine nucleotide-sensitive binding state in washed membrane preparations. In the case of the D_2 DAR, agonists typically exhibit high and low affinity-binding states in membranes, with the high affinity state reflecting the receptor coupled to its G-protein (De Lean et al., 1982; McDonald et al., 1984; Sibley et al., 1982). In contrast, antagonist binding does not promote G protein coupling and is therefore of uniform affinity and not sensitive to guanine nucleotides (De Lean et al., 1982; McDonald et al., 1984; Sibley et al., 1982). Interestingly, D_2 DAR radioligand binding studies using intact live cells, which are more representative of *in vivo* PET imaging conditions, have not revealed high affinity agonist binding states under equilibrium conditions, presumably due to the existence of endogenous GTP (Sibley et al., 1983). This is because the high affinity complex of agonist, receptor, and G protein is a transient intermediate in the catalysis of GDP-GTP exchange and G protein activation (Oldham and Hamm, 2008).

Another frequent consequence of agonist activation of G-protein coupled receptors (GPCRs) is agonist-induced receptor internalization (Marchese et al., 2008). Cell culture studies have demonstrated that large doses of agonists can cause internalization and relocation of D_2 DARs from the cell surface to intracellular compartments (Vickery and von Zastrow, 1999). Subsequent to internalization, the D_2 DAR may undergo degradation or be recycled back to the plasma membrane through mechanisms that are not yet fully understood. These findings suggest that large increases in synaptic dopamine *in vivo* might induce D_2 DAR internalization and thereby affect the binding of a PET ligand to the receptor (Ginovart et al., 2004; Goggi et al., 2007; Ito et al., 1999; Macey et al., 2004). Moreover, agonist-based probes might induce receptor internalization themselves during PET scanning experiments, thus complicating the interpretation of resulting data.

In vivo PET imaging studies, using amphetamine administration to induce dopamine release, have shown a dose-dependent decrease in the binding of D_2 DAR antagonist PET-ligands, including [^{11}C]raclopride and [^{18}F]fallypride and the SPECT ligand [^{123}I]IBZM (Breier et al., 1997; Laruelle et al., 1997; Slifstein et al., 2004). However, the decrease of radioligand binding (less than 50%) during amphetamine challenge is modest when compared to the more than 1,000-fold increase of extracellular dopamine (Breier et al., 1997; Laruelle et al., 1997; Slifstein et al., 2004). This has lead to the hypothesis that the binding of antagonist PET radioligands can only be displaced by dopamine through occupancy of the high affinity state of the receptor (Laruelle, 2000). Support for this hypothesis comes from *in vivo* studies suggesting that agonist PET ligands are more sensitive to competition from endogenous dopamine than antagonist ligands (Cumming et al., 2002; Ginovart et al., 2006; Narendran et al., 2004; Seneca et al., 2006). The differences in PET-antagonist vs. agonist radioligand binding have even been applied in studies attempting to estimate the proportion of D_2 DARs in a high affinity state *in vivo* (Hwang et al., 2005; Narendran et al., 2005; Seneca et al., 2006). One confound in this hypothesis, however, is that dopamine has always shown the ability to completely displace radiolabeled antagonist binding *in vitro*, including studies using intact cells, if sufficiently high concentrations are used (De Lean et al., 1982; Sibley et al., 1982; Sibley et al., 1983).

Interestingly, amphetamine challenge studies have also demonstrated that the specific binding of SPECT and PET-ligands remain decreased even after endogenous dopamine has

returned to basal levels, suggesting that the D_2 DARs might be internalized as a response to the amphetamine induced dopamine increase (Ginovart et al., 2006; Laruelle, 2000; Laruelle et al., 1997; Narendran et al., 2007).

Most agonists of the D_2 DAR also bind with relatively high affinity to the other subtypes of the D_2-like family, most importantly the D_3 DAR. The D_3 DAR is generally present at lower density than the D_2 DAR and has a more restricted distribution pattern in the brain. However, some CNS areas with relatively high densities of both D_2 and D_3 DAR are found in ventral putamen and nucleus accumbens, and can affect PET measurements of either receptor in these areas (Bouthenet et al., 1991; Murray et al., 1994). This is especially relevant for the novel PET-agonist [^{11}C]PHNO. Though it has been reported to have slightly higher affinity for the D_3 DAR, [^{11}C]PHNO has been utilized as a tracer in both D_2 and D_3 DAR imaging studies, based on the differential distribution of D_2 and D_3 DARs (Freedman et al., 1994; Ginovart et al., 2006; Narendran et al., 2006; Willeit et al., 2006). Thus, activity at the D_3 DAR is an important consideration for future agonist PET probes.

The goal of this study has been to characterize the pharmacology of the novel PET agonist tracer [^{11}C]MNPA. Despite previous use of [^{11}C]MNPA as a PET tracer, a full characterization of the pharmacological activity of MNPA at the D_2 and D_3 receptors has not yet been reported. Such data can be of much use in interpretation of PET imaging experiments. For example, the 5-HT_{1A} PET tracer RWAY exists as two enantiomers. It was initially demonstrated that the (*R*)-(-)-RWAY entantiomer had a much higher PET signal than its antipode, (*S*)-(+)-RWAY (Yasuno et al., 2006). Later, it was shown that (*R*)-(-)-RWAY was an antagonist whereas (*S*)-(+)-RWAY was a partial agonist (McCarron et al., 2007). Thus, pharmacological characterization of compounds for PET-imaging will facilitate a better understanding of what to expect from PET-studies utilizing new tracers.

Materials and Methods

Materials

HEK293T cells were a kind gift from Dr. Vanitha Ramakrishnan. Dulbecco's Modified Eagle Medium (DMEM) was purchased from Cellgro mediatech Inc, VA. Earles Balanced Salt Solution (EBSS), was purchased from Atlanta Biologicals, GA. Opti-MEM media and cell culture reagents were purchased from Invitrogen, Life technologies, CA. [^{3}H]cAMP, [^{3}H]methylspiperone and [^{3}H]sulpiride were purchased from PerkinElmer Life and Analytical Science, MA. [^{3}H]NPA was purchased from ViTrax radiochemicals, CA. [^{3}H]MNPA and MNPA was a kind gift from Christer Halldin, Karolinska Institutet, Stockholm, Sweden. All other compounds were purchased from Sigma-Aldrich, MO.

Cell culture

HEK293T cells were cultured in Dulbecco's Modified Eagle Medium (DMEM) containing 10% fetal bovine serum, 1 mM sodium Pyruvate, 10 μg/ml gentamicin, 50 U/ml penicillin and 50 μg/ml streptomycin. Cells were kept at 37°C in 5% CO_2. For transfection, cells were seeded in 150 mm culture dishes and transfected next day using Calcium Phosphate Transfection Kit (Clontech laboratories Inc., CA).

Radioligand Binding to Membrane Preparations

For membrane radioligand binding assays, HEK293T cells were transfected with 2 μg pcDNA3-RD_{2L} or 10μg PSRαRD3 and harvested the day after transfection. Membrane homogenates were prepared by incubating the cells in lysis buffer (5 mM Tris-HCl, 5 mM $MgCl_2$) for 10 min, followed by disruption in a glass homogenizer. The membrane fragments were then centrifuged at 34000 × g for 30 min in buffer (50 mM Tris-HCl, 1 mM

EDTA, 10 mM $MgCl_2$, pH 7.4) followed by a second resuspension and centrifugation step. The pellets were resuspended in binding buffer (50 mM Tris-HCl, 1 mM EDTA, 10 mM $MgCl_2$, 0.2 mM sodium metabisulfite), and the protein concentration was quantitated using BCA protein assay Kit (Pierce, Rockford, IL). Competition binding assays were performed in tubes containing membrane homogenate, [^{3}H]methylspiperone (final concentration ~ 0.2 nM) and competing agonists (MNPA, NPA or dopamine) in varying concentrations. Some competition studies were performed in the presence of GTP (final concentration 100 μM). Saturation binding assays were performed in tubes containing membrane homogenates and radioligand ([^{3}H]-labeled MNPA, NPA or methylspiperone) in varying concentrations. Some saturation experiments were performed in the presence of Gpp(NH)p (final concentration = 100 μM). Nonspecific binding was obtained by adding 50 μl (+)-butaclamol (final concentration 5 μM). Total binding was obtained by addition of water instead of (+)-butaclamol. The final assay volume was adjusted to 1 mL with binding buffer. After incubation at 37°C for 15 min (saturation) or one hour (competition), binding was terminated by filtration through Whatman GF/C filters on a Brandel cell harvester, followed by washing three times with 5 mL ice-cold wash buffer (50 mM Tris, pH 7.4). GF/C filters were presoaked for 2 hours in 0.3% polyethyleneimine before use. Filters were then transferred vials containing 5 ml CytoScint scintillation cocktail (ICN, Costa Mesa, CA) and quantified by liquid scintillation. All binding assays were performed in triplicates and repeated 5 times.

Radioligand Binding to Intact Cells

HEK293T Cells transfected with 2 μg pcDNA3-rD_{2L} and some were also transfected with 1 μg pcDNA3 (empty vector control) or expression constructs for arrestin2 or arrestin3 (pcDNA3-Arr2, pcDNA3-Arr3). The cells were seeded onto poly (D)-lysine coated 24 well plates at a density of 2×10^5 cell per well. One day later, the plates were washed once with 37°C Earles Balanced Salt Solution (EBSS). Binding was performed by incubation for one hour at 37°C in 500 μl EBSS containing ~2 nM [^{3}H]sulpiride, 0.2 mM sodium metabisulfite and increasing concentrations of competing agonists (MNPA, NPA or dopamine) for competition assays, or increasing concentrations of [^{3}H]sulpiride (up to ~12 nM) for saturation assays. After incubation, the binding buffer was aspirated and the plates were washed three times with 37°C EBSS. The cells were dissolved in 500 μl 1% Triton-X and transferred to vials and quantified for radioactivity by liquid scintillation spectroscopy. Specific binding was defined as the difference between total and nonspecific binding, with the latter measured in the presence of 5 μM (+)-butaclamol. In some experiments, receptor internalization was induced prior to binding by incubating the cells for 30 min at 37°C in 1 mL assay buffer (DMEM, containing 20 mM HEPES, 0.2 mM sodium metabisulfite) in the absence (control) or presence of either 10 μM dopamine or 50 nM MNPA. After agonist-treatment, the plates were washed three times with 37°C EBSS. All binding assays were performed in duplicate and repeated 4-6 times.

cAMP Accumulation Assay

HEK293T cells were transfected with 30 μg pcDNA3-rD_{2L} expressing rat D_{2L} DAR or the combination of 30 μg pcSRα-rD_3 expressing rat D_3 DAR and 0.1 μg pcIS2-rAC5 expressing rat adenylate cyclase type 5 (AC-V). The cells were then seeded in poly (D)-lysine coated 24 well plates at a density of 1.5×10^5 cells per well. One day later, the cAMP assay was performed by incubating the cells for 10 min at 37°C with increasing concentrations of agonists (MNPA, NPA or dopamine) in 400 μl assay buffer (DMEM, 20 mM HEPES, 3 μM forskolin, 30 μM RO-20-1724, 10 μM propranolol, 0.2 mM sodium metabisulfite). After incubation, buffer was removed and the cells were lysed with 200 μl 3% perchloric acid. Plates were left on ice for 30 min and the cells were neutralized with 80 μl per well $KHCO_3$. After 10 min, plates were centrifuged for 10 min at 1000 × g, and the lysate was assayed for

cAMP production, as described previously (Watts and Neve, 1996). Briefly, 50 μl cell lysate was added to reaction tubes containing 50 μl [^{3}H]cAMP (3 nM) and 250 μl protein kinase A and then incubated on ice for 90 min. The assay was terminated by the addition of 250 μl charcoal solution to each tube followed by 10 min incubation on ice and centrifugation at 2000 × g for 20 min. Radioactivity in 200 μl of the supernatant was measured by liquid scintillation spectroscopy. The concentration of cAMP was determined from a standard curve using 0.1 to 27 pmol cAMP. All experiments were performed in duplicates and repeated 3-4 times. Data were analyzed with GraphPad Prism software (GraphPad Software, Inc. CA).

Confocal Microscopy

HEK293 cells transfected with 1 μg PCIN4 expressing D_{2L}-YFP and 0.5 μg pCDNA3-Arr3 or 0.5 μg pCDNA3-Arr2 were seeded in 35 mm glass bottom culture dishes (MatTeK Corporation, MA) at a density of 2×10^5 cells per dish. The next day, cells were washed once with 37°C EBSS and covered with 1 ml Opti-MEM media. Confocal microscopy was performed at room temperature and images were acquired on a confocal laser scanning microscope (LSM 5 Pascal, Carl Zeiss, Germany) at 100× magnification. A time series of confocal images were acquired over a period of ~17 min, with the first confocal image (0 min) captured right before adding 1 ml Opti-MEM containing and either dopamine (final concentration 20 μM) or MNPA (final concentration 50 nM).

Results

We were first interested in determining the functional D_2 DAR agonist properties of MNPA in comparison to the reference agonist compounds dopamine and NPA. Figure 1 shows that all three compounds dose-dependently inhibited forskolin-stimulated cAMP accumulation in D_{2L} DAR-transfected HEK293T cells. MNPA, NPA and dopamine all maximally inhibited the cAMP response by about ~80%, although both MNPA and NPA were about 50-fold more potent than dopamine (Table I). The competitive D_{2L} DAR antagonist (+)-butaclamol reduced the potencies of all three agonists 300-1,800-fold. In addition, no D_2 DAR agonist response was observed in untransfected cells (data not shown). These results demonstrate that MNPA is a potent and full agonist at the D_{2L} DAR.

We were next interested in determining if MNPA would bind as a typical agonist, by inducing high and low affinity states of the D_{2L} DAR, in competition assays in membrane preparations (De Lean et al., 1982; Sibley et al., 1982). Figure 2 shows that in the absence of GTP, the competition curves of MNPA, NPA and dopamine were all best explained by the presence of a high and a low affinity state of the receptor. The proportion of receptors configured in the high affinity state was ~24% for both MNPA and NPA, and ~33% for dopamine (Table II). In contrast, in the presence of GTP, the agonist competition curves were all best explained by a single receptor state of low affinity (Figure 2). Notably, the affinity values in the presence of GTP are similar to the Ki values for the low affinity state in the absence of GTP. Overall, the Ki values for MNPA and NPA were ~200-1000-fold lower than dopamine, suggesting high potency and selectivity to D_{2L} DAR (Table II). These results further confirm that MNPA interacts with the D_{2L} DAR in an agonist-specific fashion.

Previously Sibley et al. (1983) have suggested that the high affinity state of the D_2 receptor is undetectable in intact cell binding assays, therefore, we were interested in evaluating agonist competition on cell surface bound receptors in intact HEK293T cells. This was accomplished by using the hydrophilic antagonist, [^{3}H]sulpiride, which does not penetrate the cell membrane and is thus restricted to bind the receptors on the cell surface (Namkung and Sibley, 2004). Figure 3 shows that, with intact cells, the agonist competition curves

were all best explained by a single receptor state of low affinity. As with the membrane binding assays, both MNPA and NPA exhibit higher affinity than dopamine. Interestingly, the Hill co-efficients of the MNPA and NPA competition curves were rather steep, which might be due to insufficient wash-out of these lipophilic synthetic agonists. Overall, these data support the notion that high affinity agonist binding is not observable in intact cell equilibrium binding assays. Notably, this assay was performed on live cells and probably best reflects the nature of agonist-receptor binding interactions observed using in vivo PET imaging experiments.

Thus far, our experiments evaluating agonist-interactions with the D_{2L} DAR have been via indirect binding assays. Consequently, we were interested in performing direct measurements of agonist-receptor binding using [^{3}H]MNPA and [^{3}H]NPA. Figure 4 shows saturation binding in membrane preparations for the agonist radioligands, along with saturation binding for the antagonist [^{3}H]methyspiperone. Adding the non-hydrolyzable GTP analog Gpp(NH)p to the assay significantly increased the Kd ~2-fold and decreased the Bmax (17-21%) of the agonists [^{3}H]MNPA and [^{3}H]NPA (Figure 4 and Table III). Similar results were observed with GTP (data not shown). In contrast, Gpp(NH)p had no effect on the binding of the antagonist ligand, [^{3}H]methylspiperone. These data suggest that only a portion the receptors are configured in the high affinity state upon MNPA and NPA occupancy, and that the binding curves in absence of Gpp(NH)p represent a mixture of high and low affinity receptor states.

Another property of most, but not all receptor agonists is to promote receptor internalization as a homeostatic mechanism of maintaining cellular responsiveness (Ferguson, 2001; Groer et al., 2007; Urban et al., 2007; Xu et al., 2007). We thus thought that it would be of interest to determine if MNPA would promote D_{2L} DAR internalization. Our first approach was to examine the loss of cell surface [^{3}H]sulpiride binding in response to agonist pretreatment as we previously reported (Namkung and Sibley, 2004). Figure 5A shows [^{3}H]sulpiride saturation binding curves to intact cells expressing D_{2L} DAR. Agonist pretreatment of the cells resulted in a loss of cell surface [^{3}H]sulpiride binding of 9% and 23% for dopamine and MNPA respectively (Figure 5 and Table IV). Notably, the loss of [^{3}H]sulpiride binding in response to dopamine pretreatment was approximately half of that observed in response to MNPA. Two members of the arrestin family are thought to mediate internalization of the D_2 receptor, either arrestin2 and/or arrestin3 – the exact isoform operative in vivo is not certain (Beaulieu et al., 2005; Macey et al., 2004). Therefore, in order to enhance the internalization of the D_{2L} receptor in HEK293 cells, we over-expressed either arrestin2 or arrestin3. As can be seen in figure 5B-C, over-expression of either arrestin2 or arrestin3 enhanced the loss of cell surface [^{3}H]sulpiride binding in response to MNPA or dopamine pretreatment. Notably, the Kd was slightly elevated in the MNPA treatment groups, suggesting incomplete washout of this hydrophobic compound. Interestingly, the internalization response to dopamine was only ~50% of the MNPA response (Table IV). These results indicate that with respect to inducing receptor internalization, MNPA is not just a full agonist, but might also be considered a “super-agonist” relative to the efficacy of dopamine.

To confirm that the loss of cell surface [^{3}H]sulpiride binding is indeed due to receptor internalization, and to further characterize this response, we used confocal microscopy to visualize the intracellular distribution of a D_{2L} DAR-yellow fluorescent protein (YFP) chimera. Figure 6 shows that under basal conditions, the D_2-YFP receptor is mostly located in the plasma membrane. After 15 min of dopamine exposure (second row of panels), however, some of the D_2-YFP fluorescence is apparent in punctuated, vesicle-like structures in the cytosol. Over-expression of either arrestin2 or arrestin3 increased receptor internalization in response to dopamine treatment and, interestingly, also promotes some receptor internalization in the basal state (Figure 6). More importantly, Figure 6 also shows

that MNPA promotes internalization of the D_2-YFP receptor and that this is enhanced with arrestin2 or arrestin3 over-expression. While this assay is not readily quantifiable, it would appear that MNPA is more effective than dopamine in reducing the cell surface receptor fluorescence (Figures 6) in agreement with the [^{3}H]-sulpiride binding assays. Taking the cAMP accumulation, receptor binding, and internalization assays together, we conclude that MNPA is a potent and full agonist at the D_2 DAR.

Because in vivo PET imaging experiments using radiolabeled MNPA as a probe might be expected to label D_3 in addition to D_2 receptors, we were interested in characterizing MNPA's interactions with the D_3 DAR as well. We initially examined D_3 DAR-mediated inhibition of cAMP accumulation. Previous studies have shown that co-expression of adenylate cyclase type 5 (AC-V) in heterologous expression systems is important to observe robust inhibition of cAMP accumulation by the D_3 DAR (Robinson and Caron, 1997). Figure 8 shows dose-response curves for MNPA and dopamine-mediated inhibition of cAMP accumulation in cells co-transfected with the D_3 DAR and AC-V. MNPA inhibited forskolin stimulated cAMP to the same extent as dopamine (42-43%), but was slightly less potent than dopamine (Figure 7A-B). The EC_{50} value of MNPA for inhibiting D_3 DAR activity was ~10-fold higher compared to its EC_{50} value at the D_2 DAR (3.4 vs. 0.3 nM, respectively). Addition of the antagonist (+)-butaclamol to the assays promoted a 100-fold reduction in potencies for both dopamine and MNPA (Figure 7A-B). These data suggest that MNPA is also a full agonist of the D_3 DAR.

We were next interested in determining if MNPA, dopamine and NPA would bind as typical agonists, to both high and low affinity states of the D_3 DAR. MNPA and NPA competition binding with [^{3}H]methylspiperone in membrane homogenates revealed complex curves best fitted to two binding sites (Figure 8A and C, Table V). Despite the existence of two apparent binding states, GTP did not alter MNPA nor NPA binding (Table V). In contrast, dopamine competition binding revealed a binding curve best fitted to a single site (Figure 8B). Moreover, addition of GTP to the binding assay did not alter the dopamine competition curve. These data suggest the existence of complex patterns of agonist binding to the D_3 DAR that differ from that of the D_{2L} DAR.

Finally, we wished to explore the agonist binding to the D_3 DAR more directly using the agonists [^{3}H]MNPA, [^{3}H]NPA, and the antagonist [^{3}H]methylspiperone for saturation binding in membrane preparations (Figure 9). As with the competition assays, the GTP analog Gpp(NH)p had no effect on saturation binding with [^{3}H]MNPA and [^{3}H]NPA (Figure 9, Table VI). As expected, Gpp(NH)p had no effect on [^{3}H]methylspiperone binding either. These data suggest that agonist binding to the D_3 DAR is complex and does not correspond to a typical binding paradigm exhibited by most agonists at GPCRs (Creese et al., 1984).

Discussion

In this study we performed a pharmacological characterization of the novel PET ligand, MNPA, using recombinant D_2 and D_3 DARs expressed in HEK293T cells. As a derivative of the DAR agonist NPA, MNPA has been suggested to have agonist properties at the D_2 DAR (Gao et al., 1990; Neumeyer et al., 1990), however, the functional activity of MNPA had not yet been characterized. We now demonstrate that MNPA exhibits full agonist efficacy at the D_{2L} DAR, as evidenced by equivalent inhibition of forskolin-stimulated cAMP accumulation when compared to dopamine. As a D_2 DAR agonist, MNPA is as potent as NPA and about 50 times more potent than dopamine. The potencies of dopamine and NPA were found to be in agreement with those previously reported (Hall and Strange, 1999; McDonald et al., 1984; Namkung and Sibley, 2004).

Competition assays in membrane preparations also showed that MNPA binds as a typical agonist by promoting both high and low affinity states of the D_{2L} DAR. It was previously suggested that the high affinity binding of an agonist reflects the G-protein activating configuration of the D_2 DAR (De Lean et al., 1982; McDonald et al., 1984; Sibley et al., 1982). This ternary complex of agonist-receptor-G protein is a transient intermediate in the activation of heterotrimeric G-proteins (Oldham and Hamm, 2008), which accumulates only in the absence of GTP. In agreement with previous studies, the MNPA-promoted high-affinity binding state from our agonist competition curves correlates well with the potency of MNPA to inhibit cAMP accumulation through the D_{2L} DAR. In addition, with all agonists, we only observed one binding state of low affinity when GTP was added to the assays.

The interactions of MNPA at the D_2 DAR were also explored more directly by using [^{3}H]MNPA saturation assays and making comparisons to the receptor binding of [^{3}H]NPA and the antagonist [^{3}H]methylspiperone. Our observations indicated that, in agreement with the competition assays, only radiolabeled agonist binding was sensitive to guanine nucleotides. Consistently, the binding of [^{3}H]MNPA and [^{3}H]NPA, but not that of the antagonist [^{3}H]methylspiperone was diminished by Gpp(NH)p. Gpp(NH)p did not completely inhibit the binding of [^{3}H]MNPA and [^{3}H]NPA, but rather decreased their maximum binding capacities (Bmax) and increased their Kd values. The percentage decrease of [^{3}H]MNPA and [^{3}H]NPA binding correlated well with the proportion of high affinity binding sites that we detected with competition assays using unlabeled MNPA and NPA. These results suggest that, in our membrane preparations, [^{3}H]MNPA and [^{3}H]NPA bind to a mixture of high and low affinity receptor states, with only the high affinity state being sensitive to guanine nucleotides. These results also serve to further confirm that MNPA interacts with the D_2 DAR in an agonist-specific fashion.

In contrast to membrane preparations, we did not detect high-affinity D_{2L} DAR binding of MNPA, NPA or dopamine with competition assays using intact cell binding assays. The absence of high affinity agonist binding in intact cells has previously been reported for the D_2 DAR (Sibley et al., 1983), whereas studies of beta-adrenergic receptors on intact cells have shown that high-affinity agonist binding can only be detected under non-equilibrium conditions (Insel et al., 1983; Toews et al., 1983). Interestingly, in intact cell binding assays, the affinity of both MNPA and NPA for the D_{2L} DAR is lower than the affinity we observe in membrane preparations in the presence of GTP, similar to that observed with adrenergic receptors (Insel et al., 1983; Toews et al., 1983). Although, high and low affinity binding sites for dopamine were recently reported by Seeman (2008) using intact pituitary cells and [^{3}H]domperidone, a radiolabeled antagonist, the [^{3}H]domperidone binding sites on these cells were not characterized as representing D_2 DARs, nor were the high affinity sites verified as representing G-protein coupled receptor complexes. Notably, ligand binding assays performed on live intact cells probably reflect *in vivo* PET conditions more accurately than binding assays in membrane preparations. Our results would thus seem to conflict with PET imaging data suggesting the identification of D_2 DAR high-affinity agonist binding states in intact brains.

After demonstrating that MNPA is a full agonist at the D_{2L} DAR using cAMP accumulation assays, and showing that it binds as a typical agonist, we investigated the ability MNPA to induce D_{2L} DAR internalization. Internalization was initially quantified by the loss of cell surface [^{3}H]sulpiride binding using intact cell assays (Namkung and Sibley, 2004). We found that MNPA treatment indeed promoted internalization of the D_2 DAR and, in fact, MNPA promoted about twice as much receptor internalization as observed in response to dopamine. In addition, we found that over-expression of the scaffolding proteins, arrestin2 or arrestin3, enhanced agonist-induced receptor internalization. These results correlate well

with previous studies showing that D_2 DARs undergo agonist-induced internalization via an arrestin and dynamin dependent mechanism, involving clathrin-coated pits (Iwata et al., 1999; Kim et al., 2001).

To confirm that the loss of cell surface D_{2L} DAR binding was indeed due to sequestration of the receptor away from the cell surface, we visualized this process using confocal fluorescence microscopy and an YFP-tagged D_2 DAR construct. Both MNPA and dopamine treatment promoted the rapid appearance of the D_2 DAR in intracellular vesicular-like structures and over-expression of arrestin2 or arrastin3 enhanced this response, in agreement with previous studies (Goggi et al., 2007; Kim et al., 2004; Sedaghat et al., 2006). Although this technique is not readily quantifiable, the internalization promoted by MNPA appeared to be greater than that promoted by dopamine in agreement with the cell surface [^{3}H]sulpiride binding assays. Interestingly, with respect to this particular agonist-induced response (internalization), MNPA appears to possess greater efficacy that the endogenous agonist dopamine. The ability of MNPA to promote profound internalization should be taken into considerations when this ligand is used for PET-studies. For example, previous PET imaging studies have estimated the *in vivo* Bmax of the D_2 DAR, using high concentrations of agonist radioligands such as [^{11}C]NPA and [^{11}C]PHNO (Ginovart et al., 2006; Narendran et al., 2005). Thus, it is possible that the high concentrations of agonist radioligands could cause significant receptor internalization, which might affect the results.

MNPA was originally developed with the purpose of using it as a D_2-selective radiolabeled agonist for PET imaging (Finnema et al., 2005; Gao et al., 1990; Seneca et al., 2006). However, most D_2 DAR ligands have significant affinity for other receptor subtypes particularly within the D_2-like subfamily. Whereas D_4 receptor expression is too low to interfere with PET imaging of the D_2 DAR, in some areas of the brain, the D_3 DAR may significantly contribute to the PET signal observed (Freedman et al., 1994; Ginovart et al., 2006; Narendran et al., 2006; Willeit et al., 2006). Consequently, it was of interest to explore the pharmacological activity of MNPA at the D_3 DAR. Measurement of the functional activity of the D_3 DAR *in vitro* has proven challenging, however, it has been reported that co-expression with adenylate cyclase type 5 leads to a robust D_3 DAR-mediated inhibition of cAMP accumulation (Robinson and Caron, 1997). Co-expression of adenylate cyclase type 5 indeed led to a measurable D_3 DAR-mediated inhibition of cAMP accumulation by both MNPA and dopamine, although the maximal level of inhibition was less than that observed with the D_{2L} DAR. Several studies suggest that agonist inhibition of cAMP accumulation through the D_3 DAR varies greatly among different cell types (Chio et al., 1994; Freedman et al., 1994; MacKenzie et al., 1994; McAllister et al., 1995; Robinson and Caron, 1997) and is usually less than that mediated by the D_2 DAR (McAllister et al., 1995). Notably, we found that MNPA inhibits forskolin-stimulated cAMP accumulation to the same extent as dopamine indicating that MNPA can be considered a full agonist at the D_3 DAR.

In membrane competition assays, we found that MNPA and NPA both bound to high and low affinity sites of the D_3 DAR. Addition of GTP to the binding assay, however, did not alter the high-affinity binding site of the D_3 DAR in contrast to what we observed with the D_{2L} DAR. Surprisingly, competition assays with dopamine showed only one binding site of the D_3 DAR, and, like MNPA and NPA, the binding was not sensitive to GTP. Interestingly, there is abundant literature noting guanine nucleotide insensitivity of agonist binding to the D_3 DAR using heterologous expression systems as well as membranes prepared from the rat olfactory tubercle (Boundy et al., 1993; Freedman et al., 1994; Levesque et al., 1992; Sokoloff et al., 1990; Vanhauwe et al., 1999). However, in some systems, guanine nucleotide sensitivity of D_3 DAR agonist binding has been observed (Castro and Strange, 1993; Chio et al., 1994; MacKenzie et al., 1994; Pilon et al., 1994). Consistent with our

competition assays, we found that saturation binding of [^{3}H]MNPA and [^{3}H]NPA to the D_3 DAR in membrane preparations was not sensitive to guanine nucleotides. These results, suggest that agonist binding to D_3 DAR is complex and not yet fully understood.

In conclusion, our current data demonstrate that the PET radioligand [^{11}C]MNPA is a full agonist at both the D_2 and D_3 DARs. As expected for an agonist ligand, MNPA promotes the formation of a high-affinity agonist binding state of the D_2 DAR in membrane preparations. However, our data does not support the detection of this transient high-affinity binding state in intact living cells at equilibrium. Further research will be required to explain the observed differences in agonist versus antagonist ligand-based PET imaging of D_2 DARs *in vivo*.

References

Beaulieu JM, Sotnikova TD, Marion S, Lefkowitz RJ, Gainetdinov RR, Caron MG. An Akt/beta-arrestin 2/PP2A signaling complex mediates dopaminergic neurotransmission and behavior. Cell. 2005; 122(2):261–273. [PubMed: 16051150]

Boundy VA, Luedtke RR, Gallitano AL, Smith JE, Filtz TM, Kallen RG, Molinoff PB. Expression and characterization of the rat D3 dopamine receptor: pharmacologic properties and development of antibodies. J Pharmacol Exp Ther. 1993; 264(2):1002–1011. [PubMed: 8437101]

Bouthenet ML, Souil E, Martres MP, Sokoloff P, Giros B, Schwartz JC. Localization of dopamine D3 receptor mRNA in the rat brain using in situ hybridization histochemistry: comparison with dopamine D2 receptor mRNA. Brain Res. 1991; 564(2):203–219. [PubMed: 1839781]

Breier JI, Mullani NA, Thomas AB, Wheless JW, Plenger PM, Gould KL, Papanicolaou A, Willmore LJ. Effects of duration of epilepsy on the uncoupling of metabolism and blood flow in complex partial seizures. Neurology. 1997; 48(4):1047–1053. [PubMed: 9109898]

Castro SW, Strange PG. Coupling of D2 and D3 dopamine receptors to G-proteins. FEBS Lett. 1993; 315(3):223–226. [PubMed: 8422910]

Chio CL, Lajiness ME, Huff RM. Activation of heterologously expressed D3 dopamine receptors: comparison with D2 dopamine receptors. Mol Pharmacol. 1994; 45(1):51–60. [PubMed: 8302280]

Creese I, Sibley DR, Leff SE. Agonist interactions with dopamine receptors: focus on radioligand-binding studies. Fed Proc. 1984; 43(13):2779–2784. [PubMed: 6383871]

Cumming P, Gillings NM, Jensen SB, Bjarkam C, Gjedde A. Kinetics of the uptake and distribution of the dopamine D(2,3) agonist (R)-N-[1-(11)C]n-propylnorapomorphine in brain of healthy and MPTP-treated Gottingen miniature pigs. Nucl Med Biol. 2003; 30(5):547–553. [PubMed: 12831994]

Cumming P, Wong DF, Gillings N, Hilton J, Scheffel U, Gjedde A. Specific binding of [(11)C]raclopride and N-[(3)H]propyl-norapomorphine to dopamine receptors in living mouse striatum: occupancy by endogenous dopamine and guanosine triphosphate-free G protein. J Cereb Blood Flow Metab. 2002; 22(5):596–604. [PubMed: 11973432]

De Lean A, Kilpatrick BF, Caron MG. Dopamine receptor of the porcine anterior pituitary gland. Evidence for two affinity states discriminated by both agonists and antagonists. Mol Pharmacol. 1982; 22(2):290–297. [PubMed: 7144730]

Ferguson SS. Evolving concepts in G protein-coupled receptor endocytosis: the role in receptor desensitization and signaling. Pharmacol Rev. 2001; 53(1):1–24. [PubMed: 11171937]

Finnema SJ, Seneca N, Farde L, Shchukin E, Sovago J, Gulyas B, Wikstrom HV, Innis RB, Neumeyer JL, Halldin C. A preliminary PET evaluation of the new dopamine D2 receptor agonist [11C]MNPA in cynomolgus monkey. Nucl Med Biol. 2005; 32(4):353–360. [PubMed: 15878504]

Freedman SB, Patel S, Marwood R, Emms F, Seabrook GR, Knowles MR, McAllister G. Expression and pharmacological characterization of the human D3 dopamine receptor. J Pharmacol Exp Ther. 1994; 268(1):417–426. [PubMed: 8301582]

Gao YG, Baldessarini RJ, Kula NS, Neumeyer JL. Synthesis and dopamine receptor affinities of enantiomers of 2-substituted apomorphines and their N-n-propyl analogues. J Med Chem. 1990; 33(6):1800–1805. [PubMed: 1971309]

Ginovart N, Galineau L, Willeit M, Mizrahi R, Bloomfield PM, Seeman P, Houle S, Kapur S, Wilson AA. Binding characteristics and sensitivity to endogenous dopamine of [11C]-(+)-PHNO, a new agonist radiotracer for imaging the high-affinity state of D2 receptors in vivo using positron emission tomography. J Neurochem. 2006; 97(4):1089–1103. [PubMed: 16606355]

Ginovart N, Wilson AA, Houle S, Kapur S. Amphetamine pretreatment induces a change in both D2-Receptor density and apparent affinity: a [11C]raclopride positron emission tomography study in cats. Biol Psychiatry. 2004; 55(12):1188–1194. [PubMed: 15184038]

Goggi JL, Sardini A, Egerton A, Strange PG, Grasby PM. Agonist-dependent internalization of D2 receptors: Imaging quantification by confocal microscopy. Synapse. 2007; 61(4):231–241. [PubMed: 17230553]

Groer CE, Tidgewell K, Moyer RA, Harding WW, Rothman RB, Prisinzano TE, Bohn LM. An opioid agonist that does not induce micro-opioid receptor--arrestin interactions or receptor internalization. Mol Pharmacol. 2007; 71(2):549–557. [PubMed: 17090705]

Hall DA, Strange PG. Comparison of the ability of dopamine receptor agonists to inhibit forskolin-stimulated adenosine 3′5′-cyclic monophosphate (cAMP) accumulation via D2L (long isoform) and D3 receptors expressed in Chinese hamster ovary (CHO) cells. Biochem Pharmacol. 1999; 58(2):285–289. [PubMed: 10423170]

Hwang DR, Narendran R, Laruelle M. Positron-labeled dopamine agonists for probing the high affinity states of dopamine subtype 2 receptors. Bioconjug Chem. 2005; 16(1):27–31. [PubMed: 15656572]

Insel PA, Mahan LC, Motulsky HJ, Stoolman LM, Koachman AM. Time-dependent decreases in binding affinity of agonists for beta-adrenergic receptors of intact S49 lymphoma cells. A mechanism of desensitization. J Biol Chem. 1983; 258(22):13597–13605. [PubMed: 6315705]

Ito K, Haga T, Lameh J, Sadee W. Sequestration of dopamine D2 receptors depends on coexpression of G-protein-coupled receptor kinases 2 or 5. Eur J Biochem. 1999; 260(1):112–119. [PubMed: 10091590]

Iwata K, Ito K, Fukuzaki A, Inaki K, Haga T. Dynamin and rab5 regulate GRK2-dependent internalization of dopamine D2 receptors. Eur J Biochem. 1999; 263(2):596–602. [PubMed: 10406971]

Kim KM, Valenzano KJ, Robinson SR, Yao WD, Barak LS, Caron MG. Differential regulation of the dopamine D2 and D3 receptors by G protein-coupled receptor kinases and beta-arrestins. J Biol Chem. 2001; 276(40):37409–37414. [PubMed: 11473130]

Kim SJ, Kim MY, Lee EJ, Ahn YS, Baik JH. Distinct regulation of internalization and mitogen-activated protein kinase activation by two isoforms of the dopamine D2 receptor. Mol Endocrinol. 2004; 18(3):640–652. [PubMed: 14684845]

Laruelle M. Imaging synaptic neurotransmission with in vivo binding competition techniques: a critical review. J Cereb Blood Flow Metab. 2000; 20(3):423–451. [PubMed: 10724107]

Laruelle M, Iyer RN, al-Tikriti MS, Zea-Ponce Y, Malison R, Zoghbi SS, Baldwin RM, Kung HF, Charney DS, Hoffer PB, Innis RB, Bradberry CW. Microdialysis and SPECT measurements of amphetamine-induced dopamine release in nonhuman primates. Synapse. 1997; 25(1):1–14. [PubMed: 8987142]

Levesque D, Diaz J, Pilon C, Martres MP, Giros B, Souil E, Schott D, Morgat JL, Schwartz JC, Sokoloff P. Identification, characterization, and localization of the dopamine D3 receptor in rat brain using 7-[3H]hydroxy-N,N-di-n-propyl-2-aminotetralin. Proc Natl Acad Sci U S A. 1992; 89(17):8155–8159. [PubMed: 1518841]

Macey TA, Gurevich VV, Neve KA. Preferential Interaction between the dopamine D2 receptor and Arrestin2 in neostriatal neurons. Mol Pharmacol. 2004; 66(6):1635–1642. [PubMed: 15361545]

MacKenzie RG, VanLeeuwen D, Pugsley TA, Shih YH, Demattos S, Tang L, Todd RD, O'Malley KL. Characterization of the human dopamine D3 receptor expressed in transfected cell lines. Eur J Pharmacol. 1994; 266(1):79–85. [PubMed: 7907989]

Marchese A, Paing MM, Temple BR, Trejo J. G protein-coupled receptor sorting to endosomes and lysosomes. Annu Rev Pharmacol Toxicol. 2008; 48:601–629. [PubMed: 17995450]

McAllister G, Knowles MR, Ward-Booth SM, Sinclair HA, Patel S, Marwood R, Emms F, Patel S, Smith A, Seabrook GR, et al. Functional coupling of human D2, D3, and D4 dopamine receptors in HEK293 cells. J Recept Signal Transduct Res. 1995; 15(1-4):267–281. [PubMed: 8903944]

McCarron JA, Zoghbi SS, Shetty HU, Vermeulen ES, Wikstrom HV, Ichise M, Yasuno F, Halldin C, Innis RB, Pike VW. Synthesis and initial evaluation of [11C](R)-RWAY in monkey-a new, simply labeled antagonist radioligand for imaging brain 5-HT1A receptors with PET. Eur J Nucl Med Mol Imaging. 2007; 34(10):1670–1682. [PubMed: 17579853]

McDonald WM, Sibley DR, Kilpatrick BF, Caron MG. Dopaminergic inhibition of adenylate cyclase correlates with high affinity agonist binding to anterior pituitary D2 dopamine receptors. Mol Cell Endocrinol. 1984; 36(3):201–209. [PubMed: 6540722]

Mukherjee J, Narayanan TK, Christian BT, Shi B, Yang ZY. Binding characteristics of high-affinity dopamine D2/D3 receptor agonists, 11C-PPHT and 11C-ZYY-339 in rodents and imaging in non-human primates by PET. Synapse. 2004; 54(2):83–91. [PubMed: 15352133]

Murray AM, Ryoo HL, Gurevich E, Joyce JN. Localization of dopamine D3 receptors to mesolimbic and D2 receptors to mesostriatal regions of human forebrain. Proc Natl Acad Sci U S A. 1994; 91(23):11271–11275. [PubMed: 7972046]

Namkung Y, Sibley DR. Protein kinase C mediates phosphorylation, desensitization, and trafficking of the D2 dopamine receptor. J Biol Chem. 2004; 279(47):49533–49541. [PubMed: 15347675]

Narendran R, Hwang DR, Slifstein M, Hwang Y, Huang Y, Ekelund J, Guillin O, Scher E, Martinez D, Laruelle M. Measurement of the proportion of D2 receptors configured in state of high affinity for agonists in vivo: a positron emission tomography study using [11C]N-propyl-norapomorphine and [11C]raclopride in baboons. J Pharmacol Exp Ther. 2005; 315(1):80–90. [PubMed: 16014571]

Narendran R, Hwang DR, Slifstein M, Talbot PS, Erritzoe D, Huang Y, Cooper TB, Martinez D, Kegeles LS, Abi-Dargham A, Laruelle M. In vivo vulnerability to competition by endogenous dopamine: comparison of the D2 receptor agonist radiotracer (-)-N-[11C]propyl-norapomorphine ([11C]NPA) with the D2 receptor antagonist radiotracer [11C]-raclopride. Synapse. 2004; 52(3): 188–208. [PubMed: 15065219]

Narendran R, Slifstein M, Guillin O, Hwang Y, Hwang DR, Scher E, Reeder S, Rabiner E, Laruelle M. Dopamine (D2/3) receptor agonist positron emission tomography radiotracer [11C]-(+)-PHNO is a D3 receptor preferring agonist in vivo. Synapse. 2006; 60(7):485–495. [PubMed: 16952157]

Narendran R, Slifstein M, Hwang DR, Hwang Y, Scher E, Reeder S, Martinez D, Laruelle M. Amphetamine-induced dopamine release: duration of action as assessed with the D2/3 receptor agonist radiotracer (-)-N-[(11)C]propyl-norapomorphine ([11C]NPA) in an anesthetized nonhuman primate. Synapse. 2007; 61(2):106–109. [PubMed: 17117423]

Neumeyer JL, Gao YG, Kula NS, Baldessarini RJ. Synthesis and dopamine receptor affinity of (R)-(-)-2-fluoro-N-n-propylnorapomorphine: a highly potent and selective dopamine D2 agonist. J Med Chem. 1990; 33(12):3122–3124. [PubMed: 2147956]

Oldham WM, Hamm HE. Heterotrimeric G protein activation by G-protein-coupled receptors. Nat Rev Mol Cell Biol. 2008; 9(1):60–71. [PubMed: 18043707]

Pilon C, Levesque D, Dimitriadou V, Griffon N, Martres MP, Schwartz JC, Sokoloff P. Functional coupling of the human dopamine D3 receptor in a transfected NG 108-15 neuroblastoma-glioma hybrid cell line. Eur J Pharmacol. 1994; 268(2):129–139. [PubMed: 7957635]

Robinson SW, Caron MG. Selective inhibition of adenylyl cyclase type V by the dopamine D3 receptor. Mol Pharmacol. 1997; 52(3):508–514. [PubMed: 9281614]

Sedaghat K, Nantel MF, Ginsberg S, Lalonde V, Tiberi M. Molecular characterization of dopamine D2 receptor isoforms tagged with green fluorescent protein. Mol Biotechnol. 2006; 34(1):1–14. [PubMed: 16943566]

Seeman P. Dopamine D2(High) receptors on intact cells. Synapse. 2008; 62(4):314–318. [PubMed: 18241049]

Seneca N, Finnema SJ, Farde L, Gulyas B, Wikstrom HV, Halldin C, Innis RB. Effect of amphetamine on dopamine D2 receptor binding in nonhuman primate brain: a comparison of the agonist radioligand [11C]MNPA and antagonist [11C]raclopride. Synapse. 2006; 59(5):260–269. [PubMed: 16416444]

Sibley DR, De Lean A, Creese I. Anterior pituitary dopamine receptors. Demonstration of interconvertible high and low affinity states of the D-2 dopamine receptor. J Biol Chem. 1982; 257(11):6351–6361. [PubMed: 6176582]

Sibley DR, Mahan LC, Creese I. Dopamine receptor binding on intact cells. Absence of a high-affinity agonist-receptor binding state. Mol Pharmacol. 1983; 23(2):295–302. [PubMed: 6835198]

Slifstein M, Narendran R, Hwang DR, Sudo Y, Talbot PS, Huang Y, Laruelle M. Effect of amphetamine on [(18)F]fallypride in vivo binding to D(2) receptors in striatal and extrastriatal regions of the primate brain: Single bolus and bolus plus constant infusion studies. Synapse. 2004; 54(1):46–63. [PubMed: 15300884]

Sokoloff P, Giros B, Martres MP, Bouthenet ML, Schwartz JC. Molecular cloning and characterization of a novel dopamine receptor (D3) as a target for neuroleptics. Nature. 1990; 347(6289):146–151. [PubMed: 1975644]

Toews ML, Harden TK, Perkins JP. High-affinity binding of agonists to beta-adrenergic receptors on intact cells. Proc Natl Acad Sci U S A. 1983; 80(12):3553–3557. [PubMed: 6134286]

Urban JD, Vargas GA, von Zastrow M, Mailman RB. Aripiprazole has functionally selective actions at dopamine D2 receptor-mediated signaling pathways. Neuropsychopharmacology. 2007; 32(1):67–77. [PubMed: 16554739]

Vanhauwe JF, Fraeyman N, Francken BJ, Luyten WH, Leysen JE. Comparison of the ligand binding and signaling properties of human dopamine D(2) and D(3) receptors in Chinese hamster ovary cells. J Pharmacol Exp Ther. 1999; 290(2):908–916. [PubMed: 10411608]

Vickery RG, von Zastrow M. Distinct dynamin-dependent and -independent mechanisms target structurally homologous dopamine receptors to different endocytic membranes. J Cell Biol. 1999; 144(1):31–43. [PubMed: 9885242]

Watts VJ, Neve KA. Sensitization of endogenous and recombinant adenylate cyclase by activation of D2 dopamine receptors. Mol Pharmacol. 1996; 50(4):966–976. [PubMed: 8863843]

Willeit M, Ginovart N, Kapur S, Houle S, Hussey D, Seeman P, Wilson AA. High-affinity states of human brain dopamine D2/3 receptors imaged by the agonist [11C]-(+)-PHNO. Biol Psychiatry. 2006; 59(5):389–394. [PubMed: 16373068]

Wilson AA, McCormick P, Kapur S, Willeit M, Garcia A, Hussey D, Houle S, Seeman P, Ginovart N. Radiosynthesis and evaluation of [11C]-(+)-4-propyl-3,4,4a,5,6,10b-hexahydro-2H-naphtho[1,2-b][1,4]oxazin-9 -ol as a potential radiotracer for in vivo imaging of the dopamine D2 high-affinity state with positron emission tomography. J Med Chem. 2005; 48(12):4153–4160. [PubMed: 15943487]

Xu ZQ, Zhang X, Scott L. Regulation of G protein-coupled receptor trafficking. Acta Physiol (Oxf). 2007; 190(1):39–45. [PubMed: 17428231]

Yasuno F, Zoghbi SS, McCarron JA, Hong J, Ichise M, Brown AK, Gladding RL, Bacher JD, Pike VW, Innis RB. Quantification of serotonin 5-HT1A receptors in monkey brain with [11C](R)-(-)-RWAY. Synapse. 2006; 60(7):510–520. [PubMed: 16952161]

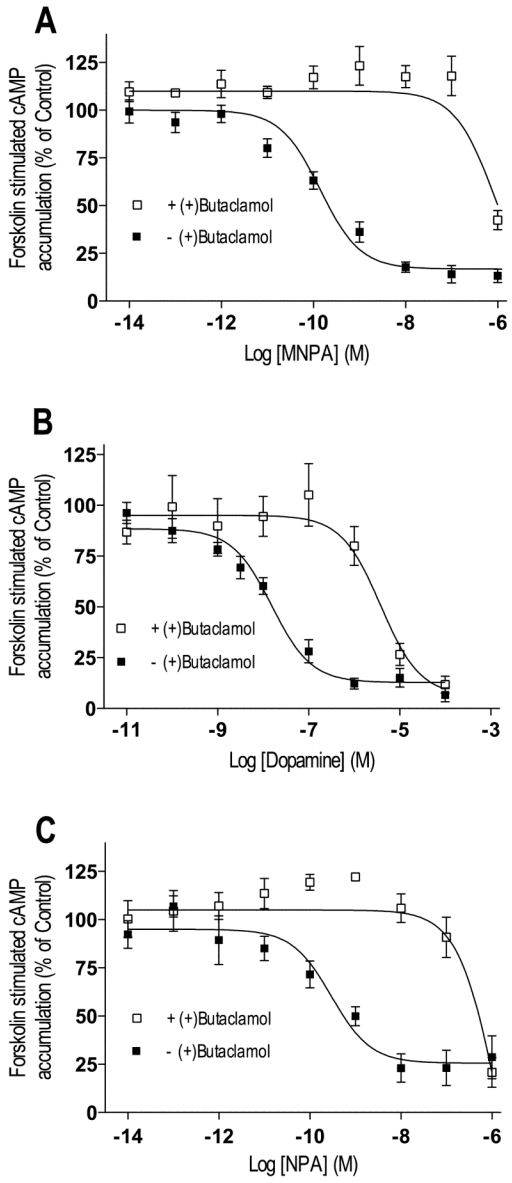

Fig. 1.

Agonist inhibition of forskolin-stimulated cAMP accumulation in HEK293T cells expressing D_{2L} DAR. Cells were incubated for 10 min at 37°C in media containing 3 μM forskolin and increasing concentrations of agonists. After incubation, the cells were assayed for cAMP accumulation as described in the methods. The agonists MNPA (**A**), dopamine (**B**) and NPA (**C**) potently inhibited forskolin-stimulated cAMP accumulation (■). Addition of 1 μM (+)-butaclamol to the assays promoted a 300-1800-fold shift in the dose-response curves to lower potencies (□). All graphs are means ± SEM from 3-4 experiments performed in duplicate. Results are summarized in table I.

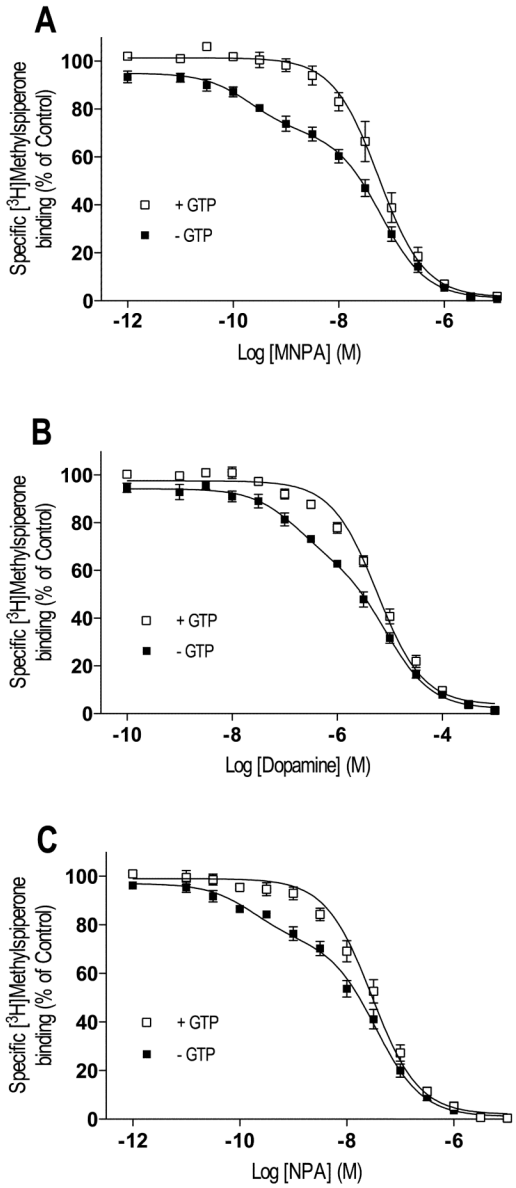

Fig. 2.

Agonist competition of [^{3}H]methylspiperone binding in membrane homogenates from HEK293T cells expressing D_{2L} DAR. Membrane homogenates were incubated for 1 hour at 37°C in buffer with [^{3}H]-methylspiperone (~0.2 nM) and increasing concentrations of the agonists MNPA (**A**), dopamine (**B**) and NPA (**C**). In the absence of GTP (■), agonist competition curves were best explained by two binding sites of high and low affinity. In the presence of 100 μM GTP (□), agonist competition curves were best explained by a single binding site of low affinity. All graphs are means ± SEM from 5 experiments performed in triplicate. Results are summarized in table II.

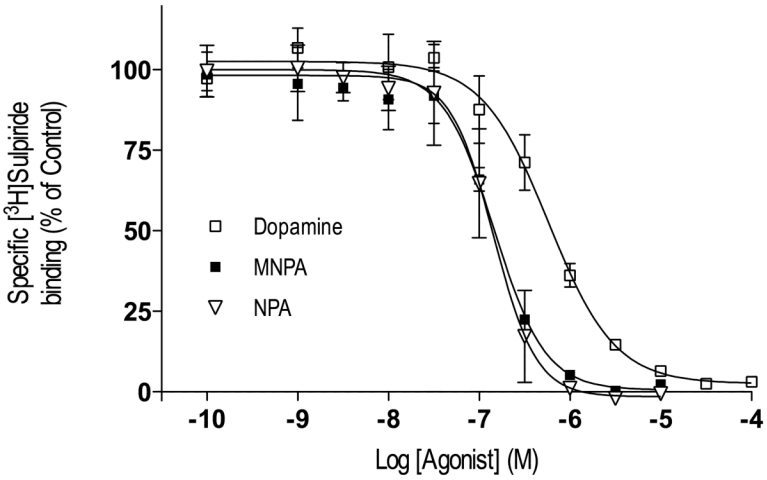

Fig. 3.

Agonist competition of cell surface [^{3}H]sulpiride binding in intact cells. HEK293T cells expressing D_{2L} DAR were incubated for 1 hour at 37°C in buffer with [^{3}H]sulpiride (~2 nM) and increasing concentrations of the agonists MNPA, dopamine and NPA. All competition curves were best explained by a single binding site of low affinity. The average Ki values were 109 ± 52, 389 ± 65and 94 ± 52 nM and hill coefficients of 1.7 ± 0.2, 1.1 ± 0.1, and 1.5 ± 0.2 for MNPA, dopamine and NPA respectively. All graphs are means ± SEM from 5 experiments performed in duplicate. An F test revealed that the hill coefficients for the three agonists were not statistically different: dopamine vs. MNPA ($p = 0.17$), dopamine vs. NPA ($p = 0.37$), and NPA vs. MNPA ($p = 0.74$).

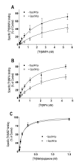

Fig. 4.

Saturation binding with [^{3}H]MNPA, [^{3}H]NPA and [^{3}H]methylspiperone in membrane homogenates from HEK293T cells expressing D_{2L} DAR. Membrane homogenates were incubated for 15 min at 37°C in assay buffer with increasing concentrations of [^{3}H]MNPA, [^{3}H]NPA or [^{3}H]methylspiperone in the absence (■) or presence (□) of GppNHp. Addition of 100 μM GppNHp to the assay caused a significant reduction in B_{max} and an increase in K_d for [^{3}H]MNPA and [^{3}H]NPA (**A-B**). The antagonist [^{3}H]-methylspiperone was not sensitive to GppNHp (**C**). All graphs are means ± SEM from 5 experiments performed in triplicate. Average values are summarized in table III.

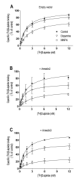

Fig. 5.

Agonist induced internalization of D_{2L} DAR in intact cells measured by decreased cell surface binding of [^{3}H]sulpiride. HEK293T cells were transfected with D_{2L} DAR and co-transfected with either empty vector (pcDNA) (**A**), or expression constructs for arrestin2 (**B**) or arrestin3 (**C**). Cells were incubated for 30 min at 37°C in either buffer only (■) or buffer containing 10 μM dopamine (∇) or 50 nM MNPA (□) prior to saturation binding with [^{3}H]sulpiride. Both MNPA and dopamine caused a decrease in cell surface [^{3}H]sulpiride binding and the decreased was enhanced by co-transfection with arrestin2 or arrestin3. All graphs are means ± SEM from 4-6 experiments performed in triplicate. Average values are summarized in table IV.

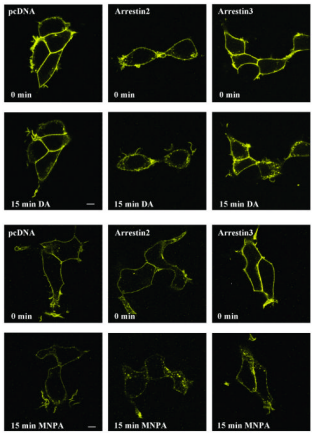

Fig. 6.

Agonist-induced receptor internalization assessed via confocal microscopy. HEK293T cells were transfected with D_{2L}-YFP and cotransfected with either empty vector (pcDNA), or expression constructs for arrestin2 or arrestin3. Cells were kept in media at room temperature and treated with either 10 μM dopamine or 50 nM MNPA. Confocal microscopy was performed as described in the Methods. Confocal images were captured right before (0 min-upper panels) and 15 min (lower panels) after either dopamine or MNPA were added. Bar = 10 μm.

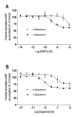

Fig. 7.

Agonist inhibition of forskolin-stimulated cAMP accumulation in HEK293T cells expressing D_3 DAR and adenylate cyclase type 5. Cells were incubated for 10 min at 37°C in media containing 3 μM forskolin and increasing concentrations of agonists. After incubation, the cells were assayed for cAMP accumulation as described in the methods in the absence (■) or presence (□) of (+)-butaclamol. The agonists MNPA (**A**), dopamine (**B**) partially inhibited (42-43%) forskolin stimulated cAMP accumulation with IC_{50} values of 3.43 nM and 1.1 nM respectively. Addition of 10 μM (+)butaclamol to the assay shifted the dose-response curves to 100 fold lower potencies (IC_{50} = 253 nM and 146 nM for MNPA and dopamine respectively). All graphs are means ± SEM from 3-4 experiments performed in duplicate.

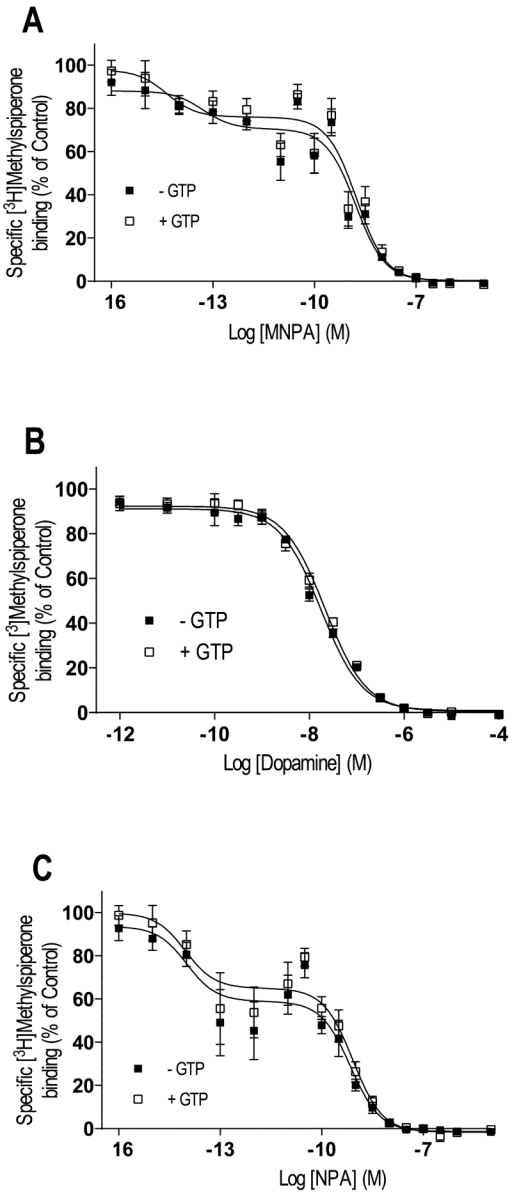

Fig.8.

Agonist competition of [^{3}H]methylspiperone binding in membrane homogenates from HEK293T cells expressing the D_3 DAR. Membrane homogenates were incubated with [^{3}H]methylspiperone (~0.2 nM) and increasing concentrations of the agonists MNPA, dopamine and NPA. Competition binding was performed in the presence (□) and absence (■) of 100 μM GTP. Although competition binding with the synthetic agonists MNPA (**A**) and NPA (**C**) were best explained by a two-site binding curve, the dopamine curve (**B**) was best explained by a one-site binding curve and none of the agonists competition binding were sensitive to GTP. All graphs are means ± SEM from 5 experiments performed in triplicate. Average values are summarized in table V.

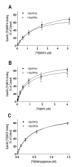

Fig. 9.

Saturation binding with [^{3}H]MNPA, [^{3}H]NPA and [^{3}H]methylspiperone in membrane homogenates from HEK293T cells expressing D_3 DAR. Membrane homogenates were incubated for 15 min at 37°C in assay buffer with increasing concentrations of [^{3}H]MNPA, [^{3}H]NPA and [^{3}H]methylspiperone in the absence (■) or presence (□) of GppNHp. Addition of 100 μM GppNHp did not cause any significant changes in the binding of any of the radioligands. All graphs are means ± SEM from 5 experiments performed in triplicate. Average values are summarized in table VI.

Table I

Agonist inhibition of forskolin-stimulated cAMP accumulation in HEK293T cells expressing D_{2L} DAR.

Agonist	% Maximum inhibition	IC_{50} (nM)	IC_{50} (+)-butaclamol (nM)
MNPA	82 ± 3	0.33 ± 0.26	619 ± 34
Dopamine	85 ± 3	15.6 ± 1.75	3920 ± 944
NPA	72 ± 8	0.37 ± 0.09	296 ± 55

Values are means ± SEM from 3-4 experiments performed in duplicate.

Table II

Agonist competition of [^{3}H]methylspiperone binding in membranes from cells expressing D_{2L} DAR.

Agonist	K_{iH} (nM)	K_{iL} (nM)	% R_H
MNPA	0.09 ± 0.02	16.9 ± 3.2	24 ± 1
MNPA + GTP		13.7 ± 3.3	
Dopamine	50.5 ± 26.89	1770 ± 310	33 ± 3
Dopamine + GTP		1270 ± 116	
NPA	0.06 ± 0.03	8.9 ± 1.8	24 ± 1
NPA + GTP		7.9 ± 1.6	

Values are means ± SEM from 5 experiments performed in triplicate. R_H: Percentage of receptors configured in the GTP sensitive high-affinity state. An F test (comparison of curves) revealed that %R_H values for the three agonists were not significantly different: dopamine vs. MNPA ($p = 0.20$), dopamine vs. NPA ($p = 0.22$), and MNPA vs. NPA ($p = 0.97$).

Table III

Saturation binding with [^{3}H]MNPA, [^{3}H]NPA and [^{3}H]methylspiperone in membranes from cells expressing D_{2L} DAR.

Agonist	Kd (nM)	B_{max} (pmol/mg)	% decrease of B_{max}
MNPA	2.21 ± 0.31	1.18 ± 0.17	
MNPA + Gpp(NH)p	4.46 ± 0.96*	0.92 ± 0.25*	21 ± 9
NPA	1.17 ± 0.11	0.93 ± 0.03	
NPA + Gpp(NH)p	2.38 ± 0.29*	0.79 ± 0.05*	17 ± 5
MSP	0.09 ± 0.01	1.04 ± 0.03	
MSP + Gpp(NH)p	0.10 ± 0.01	1.08 ± 0.03	

Values are means ± SEM from 5 experiments performed in triplicate.

*Gpp(NH)p significantly decreased the B_{max} values and increased the Kd values of [^{3}H]MNPA and [^{3}H]NPA, compared to controls ($p<0.001$, F-test).

Table IV

Agonist induced internalization of D_{2L} DAR in intact cells measured by decreased cell surface binding of [^{3}H]sulpiride.

Transfection	Agonist	Kd (nM)	B_{max} (fmol/10^5cells)	% decrease of B_{max}
pcDNA	Control	1.63 ± 0.28	9.07 ± 0.49	
	MNPA	2.77 ± 0.51	7.25 ± 0.53	23 ± 7
	Dopamine	1.54 ± 0.28	8.29 ± 0.48	9 ± 4
Arrestin2	Control	1.85 ± 0.51	6.64 ± 0.62	
	MNPA	2.17 ± 0.66	3.00 ± 0.33	53 ± 2
	Dopamine	1.23 ± 0.34	4.22 ± 0.38	34 ± 7
Arrestin3	Control	1.46 ± 0.25	7.97 ± 0.44	
	MNPA	3.14 ± 0.72	2.75 ± 0.27	68 ± 8
	Dopamine	1.35 ± 0.31	5.55 ± 0.40	29 ± 7

Values are means ± SEM from 4-6 experiments performed in duplicate.

Table V

Agonist competition of [^{3}H]methylspiperone binding in membranes from cells expressing D_3 DAR.

Agonist	K_{iH} (fM)	K_{iL} (nM)
MNPA	32.6 ± 16.1	1.02 ± 0.2
MNPA + GTP	2.66 ± 0.2	1.09 ± 1.7
Dopamine		11.2 ± 2.1
Dopamine + GTP		13.7 ± 3.9
NPA	6.07 ± 3.6	0.44 ± 0.1
NPA + GTP	5.53 ± 0.7	0.52 ± 0.3

Values are means ± SEM from 5 experiments performed in triplicate.

Table VI

Saturation binding with [^{3}H]MNPA, [^{3}H]NPA and [^{3}H]methylspiperone in membranes from cells expressing the D_3 DAR.

Agonist	Kd (nM)	B_{max} (pmol/mg)
MNPA	2.02 ± 0.67	3.24 ± 0.48
MNPA + Gpp(NH)p	1.57 ± 0.51	2.57 ± 0.34
NPA	0.61 ± 0.20	2.00 ± 0.22
NPA + Gpp(NH)p	0.58 ± 0.20	1.82 ± 0.21
MSP	0.39 ± 0.07	1.48 ± 0.10
MSP + Gpp(NH)p	0.47 ± 0.08	1.54 ± 0.10

Values are means ± SEM from 5 experiments performed in triplicate.